Rigid plastic analysis for bearing capacity of strip footings subjected to combined loads

Capacité portante d'une fondation superficielle soumise à les charges combinées de l'analyse rigido-plastique

S. Kobayashi & R. Izawa
Kyoto University, Japan

ABSTRACT

Bearing capacity characteristics of a strip footing subjected to combined loads are investigated in this paper. In the framework of rigid plastic analysis, interactions along the interface of a footing and a soil, such as contact/separation and slippage, are adequately implemented in a formulation of a hybrid type rigid plastic finite element method as inequality constraint conditions. According to the numerical results, the importance of the interfacial friction is highlighted for the horizontal resistance. The influence of self weight of a soil mass on a shape of a bearing capacity locus is also highlighted.

RÉSUMÉ

On étudie la capacité de soutien du sol sur une bande en fonction de différents poids. Dans le cadre de l'analyse d'un plastique rigide, les interactions entre la surface d'un pied et le sol (telles que le contact ou le glissement) ont été modélisées en un plastique rigide hybride grâce à la méthode des éléments finis avec des inégalités de contrainte. Les résultats numériques mettent en évidence l'importance des interactions d'interface pour la résistance horizontale. De plus, ces résultats montrent l'influence du poids et de la forme de l'objet sur la capacité de soutien du sol.

Keywords: Bearing capacity, Strip footing, Combined loads, Rigid plastic FEM, Interaction

1 INTRODUCTION

Recently, quantitative understanding of bearing capacity characteristics of strip footings subjected to combined loading conditions is increasingly required, because in many cases, shallow strip footings are selected as foundations of oil producing facilities in an ocean area and foundations of wind energy facilities, mainly due to the economic reason. Structures of those facilities are usually under severe loading conditions, such that large horizontal or moment external loads are acting on the structures.

In general, bearing capacity characteristics are simply expressed as a bearing capacity locus in the generalized load space (V, H, M/B), where V, H and M are vertical, horizontal and moment loads acting on a shallow footing with the width B, respectively. To understand the shape of a bearing capacity locus, many previous studies have been carried out both experimentally and numerically. It is widely accepted that a shape of a bearing capacity locus is a cigar-like shape as shown in Figure 1 qualitatively (For example, Bransby 2001, Hjiaj et al. 2004, Houlsby & Purzin 1999, Gottardi & Butterfield 1993, Poulos et al. 2001, Salenşon & Pecker 1995, Ukritchon et al. 1998).

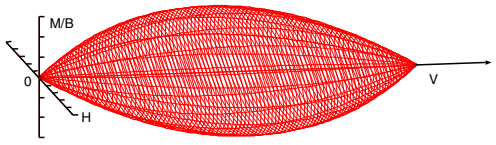

Figure 1. Schematic view of a bearing capacity locus

A mechanical property along the interface of a footing and a soil is increasingly important, if severe loading conditions such that large horizontal and/or moment loads are acting under relatively small vertical loads are considered. In such cases, interactions along the interface of a shallow footing and a soil are as important as the mechanical properties of a soil mass itself. To this end, it is necessary to implement the interactions such that contact/separation and slippages along the interface of a footing and a soil in the analysis. In addition to this, a failure of a footing structure is sometimes implemented to understand the overall bearing capacity characteristics.

Limit analysis is usually used to evaluate the ultimate bearing capacity of a footing in practical engineering, because of its simple but rigorous mathematical background. Unfortunately numerical studies such that the contact/separation and slippage along the interface of a footing and a soil are directly included can not be found in the literature. The author has proposed a hybrid type rigid plastic finite element method (Kobayashi 2005), which solve the static and kinematic conditions simultaneously in the iterative manner to achieve the optimum solution. The most advantageous point of this method is to handle the inequality constraint conditions directly in the numerical calculations. In other words, it is easy to handle that the inequality constraint conditions such as contact/separation and Coulomb's frictional law.

In this paper, extension of a hybrid type rigid plastic FEM implementing the interactions along the interface of a footing and a soil is formulated. The proposed method is then applied to a bearing capacity problem of a strip footing to investigate the bearing capacity characteristics. A mobilization mechanism of bearing capacity is also discussed. In addition, a numerical study including a mending failure of a footing structure is briefly presented.

2 FORMULATION OF BEARING CAPACITY PROBLEMS BY RIGID PLASTIC FEM

In this study, a bearing capacity problem of a shallow foundation on a flat c, phi soil illustrated in Figure 2 is investigated. Rigid plastic formulation of a bearing capacity problem in two dimension subject to combined external loads (V, H, M/B) is presented in this section, where V, H and M are vertical, horizontal and moment loads and B is a width of a footing, respectively. The positive directions of external loads are also defined in Figure 2.

In the numerical analysis, external loads $\boldsymbol{g}$ are decomposed in a constant term $\boldsymbol{g}_c$ and a variable term $\boldsymbol{g}_0$ and a load factor α as

$$\boldsymbol{g} = \boldsymbol{g}_c + \alpha \boldsymbol{g}_0. \tag{1}$$

A series of calculations are carried out for various $\boldsymbol{g}_c$ and $\boldsymbol{g}_0$ to evaluate the overall bearing capacity characteristics.

doi:10.3233/978-1-60750-031-5-626

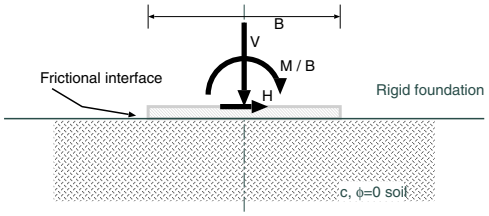

Figure 2. A target boundary value problem

2.1 *Rigid plastic modeling of interactions along the interface of soils and strip foundations*

An interface of a footing and a soil is modeled in the framework of mechanics of rigid-plasticity. Coulomb's friction law and no tensile resistance are introduced to the interface as illustrated in Figure 3. Nodal forces $\boldsymbol{t}$ at a footing are decomposed in normal components t_{ni} and tangential components t_{ti}. Concretely, Coulomb's friction law $|t_{ti}| \leq \tan\phi_{in} \cdot (-t_{ni})$ and no tensile resistance $t_{ni} \leq 0$ are simply summarized as

$$\boldsymbol{L}^T\boldsymbol{t} + \boldsymbol{k} = \boldsymbol{0},\ \boldsymbol{k} \geq \boldsymbol{0} \tag{2}$$

where $\boldsymbol{k}$ is a non-negative slack variable.

An equilibrium equation of a footing structure is expressed as

$$\boldsymbol{E}^T\boldsymbol{t} = \boldsymbol{g}_c + \alpha\boldsymbol{g}_0 \tag{3}$$

where $\boldsymbol{t}$ is a reaction force from a soil and $\boldsymbol{g}_c$ and $\boldsymbol{g}_0$ are external loads. This equilibrium condition can directly derive to a rigid motion of a footing structure based on the duality theory.

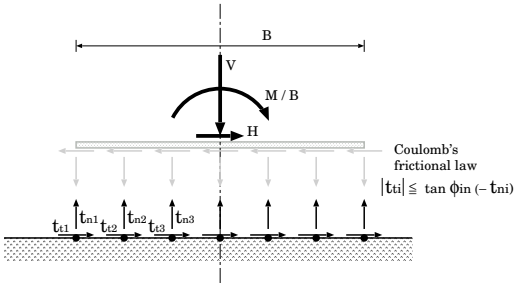

Figure 3. Rigid plastic model of an interface of a footing and a soil

2.2 *Lagrangian of bearing capacity problems with considering the interactions between soils and footings*

The lower bound method for the bearing capacity calculations is to maximize a load factor α under static constraint conditions. The Lagrangian to this method is expressed as follows,

$$L = \begin{cases} \alpha + \boldsymbol{\kappa} \cdot \left(\boldsymbol{B}^T\boldsymbol{\sigma} - \boldsymbol{H}^T\boldsymbol{t} - \boldsymbol{b} - \boldsymbol{D}_d^T\boldsymbol{p}\right) \\ \quad - \boldsymbol{\lambda} \cdot (\boldsymbol{f}(\boldsymbol{\sigma}) + \boldsymbol{s}) + \boldsymbol{s} \cdot \boldsymbol{u} \\ \quad + \boldsymbol{\zeta} \cdot \left(\boldsymbol{E}^T\boldsymbol{t} - \boldsymbol{g}_c - \alpha\boldsymbol{g}_0\right) - \boldsymbol{\xi} \cdot \left(\boldsymbol{L}^T\boldsymbol{t} + \boldsymbol{k}\right) \\ \quad + \boldsymbol{k} \cdot \boldsymbol{v} \quad \text{if } \boldsymbol{u} \geq \boldsymbol{0}, \boldsymbol{v} \geq \boldsymbol{0} \\ +\infty \quad \text{otherwise} \end{cases} \tag{4}$$

where variables $\boldsymbol{\kappa}$, $\boldsymbol{\lambda}$, $\boldsymbol{u}$, $\boldsymbol{\zeta}$, $\boldsymbol{\xi}$ and $\boldsymbol{v}$ are Lagrangian multipliers. The physical meaning of the right-hand side of Equation (4) is as follows. The first term stands for a load factor α. The second term is equilibrium equations in a soil mass where $\boldsymbol{\sigma}$, $\boldsymbol{t}$, $\boldsymbol{b}$ and $\boldsymbol{p}$ are stresses in an element, nodal forces transmitted from a footing to a soil, body forces and nodal forces on the Dirichlet boundary. The third and the fourth terms are yielding conditions of a soil mass where f is a yield function and the non-negativeness of a slack variable $\boldsymbol{s}$, respectively. The fifth term is an equilibrium in a footing structure. The sixth and seventh terms are inequality constraint conditions along the interface of a footing and a soil and the non-negativeness of a slack variable $\boldsymbol{k}$, respectively.

The upper bound method and the lower bound method are dual to each other and derived as follows,

$$\text{Upper bound method:} \quad \inf_{\boldsymbol{\kappa},\boldsymbol{\lambda},\boldsymbol{u},\boldsymbol{\zeta},\boldsymbol{\xi},\boldsymbol{v}} \left\{ \sup_{\alpha,\boldsymbol{\sigma},\boldsymbol{t},\boldsymbol{p},\boldsymbol{s},\boldsymbol{k}} L \right\} \tag{5}$$

$$\text{Lower bound method:} \quad \sup_{\alpha,\boldsymbol{\sigma},\boldsymbol{t},\boldsymbol{p},\boldsymbol{s},\boldsymbol{k}} \left\{ \inf_{\boldsymbol{\kappa},\boldsymbol{\lambda},\boldsymbol{u},\boldsymbol{\zeta},\boldsymbol{\xi},\boldsymbol{v}} L \right\} \tag{6}$$

A Difference of the ultimate capacities by both the upper bound and the lower bound methods is called a duality gap $\mathcal{G}$ and expressed as the products of non-negative variables $\boldsymbol{s}$, $\boldsymbol{\lambda}$, $\boldsymbol{k}$ and $\boldsymbol{\xi}$,

$$\mathcal{G} = \boldsymbol{s} \cdot \boldsymbol{\lambda} + \boldsymbol{k} \cdot \boldsymbol{\xi} \geq 0. \tag{7}$$

According to the duality theorem, solutions by both the upper bound and the lower bound methods coincide, if and only if the solutions are optimum. In addition, complementarity condition shown below is also satisfied,

$$\boldsymbol{S}\boldsymbol{\lambda} = \boldsymbol{\Lambda}\boldsymbol{s} = \boldsymbol{0}, \quad \boldsymbol{S} = \mathrm{diag}(s_i),\ \boldsymbol{\Lambda} = \mathrm{diag}(\lambda_i) \tag{8}$$

$$\boldsymbol{K}\boldsymbol{\xi} = \boldsymbol{\Xi}\boldsymbol{k} = \boldsymbol{0}, \quad \boldsymbol{K} = \mathrm{diag}(k_i),\ \boldsymbol{\Xi} = \mathrm{diag}(\xi_i) \tag{9}$$

2.3 *Equations satisfied by exact solutions and their solver*

The optimum solution is achieved when the solutions solved by both the upper bound method and the lower bound method coincide. Therefore, the optimum solution satisfies the constraint conditions for both the upper bound method and the lower bound method. In addition, the complementarity condition is also satisfied. All the equations satisfied by the optimum solution are shown as follows,

SOIL MASS

Equilibrium	$\boldsymbol{B}^T\boldsymbol{\sigma} - \boldsymbol{H}^T\boldsymbol{t} - \boldsymbol{b} - \boldsymbol{D}_d^T\boldsymbol{p} = \boldsymbol{0}$	(10)
Yielding	$\boldsymbol{f}(\boldsymbol{\sigma}) + \boldsymbol{s} = \boldsymbol{0}$	(11)
External work rate	$\boldsymbol{\zeta} \cdot \boldsymbol{g}_0 = 1$	(12)
Flow rule	$\boldsymbol{B}\boldsymbol{\kappa} = \left(\dfrac{\partial \boldsymbol{f}}{\partial \boldsymbol{\sigma}}\right)^T \boldsymbol{\lambda}$	(13)
Fixed boundary	$\boldsymbol{D}_d\boldsymbol{\kappa} = \boldsymbol{0}$	(14)
Complementarity	$\boldsymbol{S}\boldsymbol{\lambda} = \boldsymbol{\Lambda}\boldsymbol{s} = \boldsymbol{0},\ \boldsymbol{s} \geq \boldsymbol{0},\ \boldsymbol{\lambda} \geq \boldsymbol{0}$	(15)

FOUNDATION

Equilibrium	$\boldsymbol{E}^T\boldsymbol{t} = \boldsymbol{g}_c + \alpha\boldsymbol{g}_0$	(16)
Interface	$\boldsymbol{L}^T\boldsymbol{t} + \boldsymbol{k} = \boldsymbol{0}$	(17)
Rigid motion	$\boldsymbol{E}\boldsymbol{\zeta} = \boldsymbol{H}\boldsymbol{\kappa} + \boldsymbol{L}\boldsymbol{\xi}$	(18)
Complementarity	$\boldsymbol{K}\boldsymbol{\xi} = \boldsymbol{\Xi}\boldsymbol{k} = \boldsymbol{0},\ \boldsymbol{k} \geq \boldsymbol{0},\ \boldsymbol{\xi} \geq \boldsymbol{0}$	(19)

In this paper, primal-dual interior point method is used to solve these equations simultaneously. In this method, from the initial assumed solutions, duality gaps are gradually decreasing along the inside of a feasible region to achieve the optimum solution. Details of the numerical algorithm is illustrated in a reference (Kobayashi, 2005).

3 RESULTS OF NUMERICAL STUDIES

3.1 *Bearing capacity characteristics of weightless c, $\phi = 0$ soils*

At first, a series of numerical analysis are carried out to investigate bearing capacity characteristics of shallow foundations on

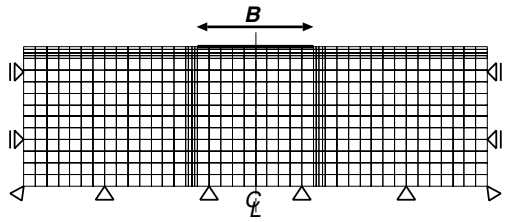

Figure 4. Finite element mesh

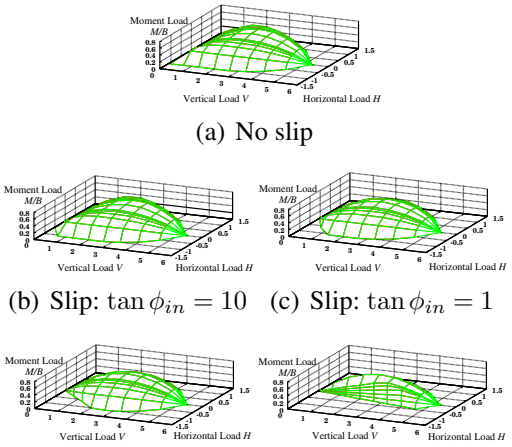

(a) No slip

(b) Slip: $\tan\phi_{in} = 10$ (c) Slip: $\tan\phi_{in} = 1$

(d) Slip: $\tan\phi_{in} = 0.5$ (e) Slip: $\tan\phi_{in} = 0.1$

Figure 5. Shape of bearing capacity loci (weightless c, $\phi = 0$ soil)

weightless c, $\phi = 0$ soils. A FEM mesh is shown in Figure 4. Numerical results are summarized as a bearing capacity locus in the loading space (V, H, M/B) shown in Figure 5. Properties along the interface of a footing and a soil are expressed as two following cases; (i) frictional interface which obeys both Coulomb's friction law with parameter $\tan\phi_{in}$ and no tensile strength and, (ii) fixed interface which shows a footing and a soil beneath it are perfectly fixed.

Cross-sectional shapes of bearing capacity loci (Figure 5)are also shown in Figure 6. In this figure, cross-sections on the zero moment load plane ($M/B = 0$), the zero horizontal load plane ($H = 0$) and the constant vertical load plane ($V/V_{\max} = 0.5$) are shown.

For less interfacial friction cases along the interface, horizontal capacity is directly dominated by the interfacial friction. However, for purely eccentric loading cases ($H = 0$), bearing capacity is independent of the interfacial friction $\tan\phi_{in}$. A cross-section of a bearing capacity locus on the $V/V_{\max} = 0.5$ plane is not symmetric to both the $M/(B \cdot V_{\max})$-axis and the $H/V_{\max}$ axis. Distortion of a cross-sectional shape is depending on the interfacial friction $\tan\phi_{in}$, but the differences decrease with the decrease of the interfacial friction angle ϕ_{in}.

3.2 *Bearing capacity characteristics of c, ϕ soils*

According to the bearing capacity formula for a surface shallow footing, bearing capacity is approximately decomposed into two terms; one is due to cohesion and the other is due to self-weight of soils. Therefore, a relative weight of these two terms is expressed as a parameter G defined as follows,

$$G = \frac{\rho g B}{2c}. \tag{20}$$

Hereafter, numerical results for a rough footing are presented and discussed.

Sizes of bearing capacity loci are larger with the increase of self-weight. Cross-sectional shapes of a bearing capacity locus

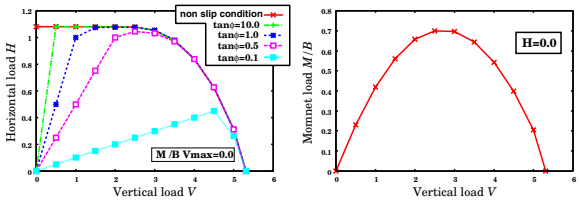

(a) On $M/B = 0$ plane (b) On $H = 0$ plane

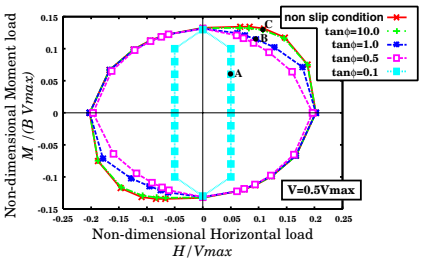

(c) On $V/V_{\max} = 0.5$ plane

Figure 6. Cross-sectional views of bearing capacity loci (weightless c, $\phi = 0$ soil)

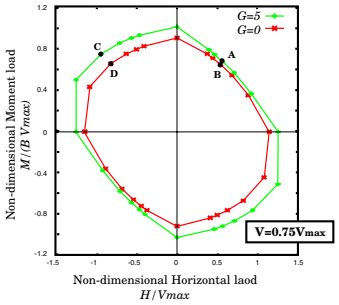

Figure 7. Cross-sectional views of bearing capacity loci (c, $\phi = 10^\circ$ soil)

of an inclined loading case (on the $M/B = 0$ plane) and an eccentric loading case (on the $H = 0$ plane) are similar to those of weightless soil cases. On the contrary, cross-sectional shapes on the $V =$ const. plane depend on the self-weight of soils.

When the self-weight of soils are considered, not only the internal dissipation rate of a plastic zone but also the external plastic work rate due to the self-weight are contributing to the bearing capacity as shown in Figure 8. In other words, more external plastic work rate due to the self-weight causes more passive pressure acting on a plastic wedge beneath a footing. Therefore, larger failure mechanism in the soil shows larger bearing capacity. For example, non-symmetry shape of a bearing capacity locus on the H-M/B cross section in $G = 5$ case can be illustrated by the this reason.

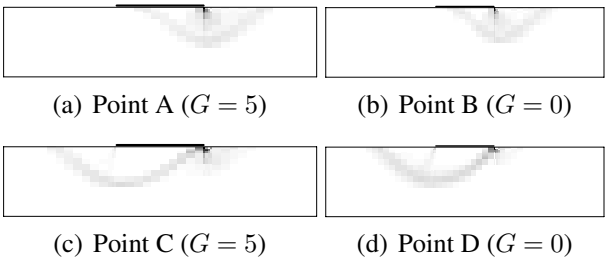

(a) Point A ($G = 5$) (b) Point B ($G = 0$)

(c) Point C ($G = 5$) (d) Point D ($G = 0$)

Figure 8. Various Failure modes of c, $\phi = 10^\circ$ soil (Points A,B,C and D are indicated in Figure 7)

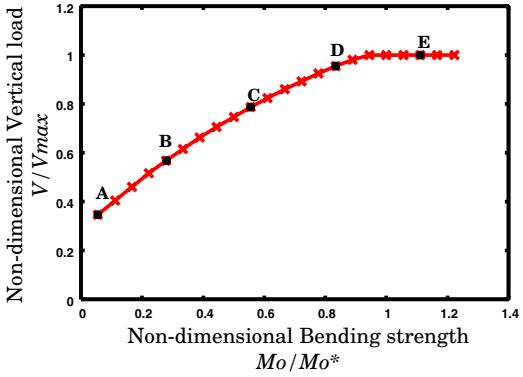

Figure 9. Relation of vertical capacity and Bending strength

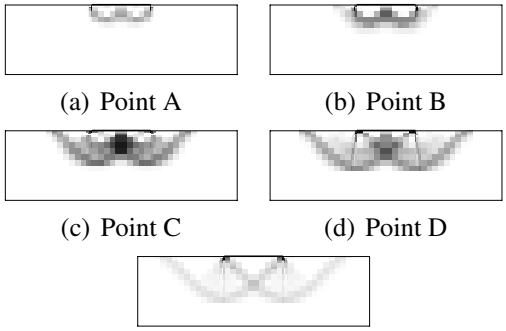

Figure 10. Distribution of internal dissipation rate (Points A ^{s}im E are indicated in Figure 9)

3.3 *Influence of bending strength of a strip foundation on bearing capacity characteristics*

It is not always satisfied the condition that a footing is rigid, especially for a case that a footing bears a larger vertical load. For such a case, as a larger bending moment occur in a footing, we should also consider bending failure of a footing. Implementation of this to the analysis is as follows. A footing structure is modeled such that rigid bars are connected with rigid-plastic bending springs. Bending moments in a footing are calculated depending on the reaction from the soil and the external load. Inequality constraints such that moments at each nodal points do not exceed the bending strength of a footing structure are added in the optimization.

For example, bearing capacity of a shallow footing on weightless c, $\phi = 0$ soils subjected to central vertical loads is illustrated in Figure 9. It can be found that dimensionless vertical capacity $V/V_{\max}$ depends on the bending strength of a footing structure Q^*, where $V_{\max}$ stands for the maximum bearing capacity for a rigid footing.

Distribution of internal dissipation rate in the soils is shown in Figure 10. For a less bending strength case, less bearing capacity is observed as only the central portion of a footing contacts to the soil and a failure mechanism is similar to Hill's mechanism . On the contrary, for a more bending strength case, a footing fully contacts to the soil and Prandtl's mechanism is found in the soil. For intermediate bending strength cases, failure mechanism is a combination of both Hill's and Prandtl's mechanisms.

It should be noted that distribution of external loads directly influence the bearing capacity, if bending of a footing structure is considered.

4 CONCLUSIONS

In this paper, a new numerical method is proposed and applied to bearing capacity problems of shallow foundations. Findings are briefly summarized as follows.

Development of a systematic solver based on hybrid type rigid plastic FEM

(1) Interactions of soils and strip footings such as contact / separation and Coulomb friction slippage are modeled as simple rigid plastic inequality constraint conditions and fully implemented into a hybrid type formulation of rigid plastic finite element method.
(2) In the similar way, bending failure of strip foundation structures is also modeled as rigid plastic inequality constraint conditions.

Bearing capacity characteristics of a strip footing subjected to combined loads

Newly proposed rigid plastic FEM is applied to the analyses of bearing capacity problems of strip footings subjected to combined loads. These numerical results are summarised as a bearing capacity locus in a generalized load domain V, H, M/B, where V, H and M are vertical, horizontal and moment loads applying to a strip footing with the width B.
(1) For weightless c, $\phi = 0$ soils, horizontal bearing capacity mainly depends on the friction along the interface of the soils and footings. Combination of horizontal and moment loads is also important and positive - positive combination (see Fig. 3) shows larger capacities. However, these differences decreases with the decrease of friction along the interface.
(2) For c, ϕ soils, to investigate the contribution of self-weight to the bearing capacity, numerical studies are carried out for two different self-weight cases. As the effect of self weight increase when the failure mechanism extend to the deeper from the surface and mobilize, the shape of non-symmetry on the H-M/B surface changes.

REFERENCES

Bransby, M.F: Failure envelopes and plastic potentials for eccentrically loaded surface footings on undrained soil, *International Journal of Numerical and Analytical Methods in Geomechanics*, 25, 329–346, 2001.

Hjiaj, M., Lyamin, A.V. & Sloan, S.W.: Bearing capacity of a cohesive-frictional soil under non-eccentric inclined loading, *Computers and Geotechnics*, 31, 491–516, 2004.

Houlsby, G.T. & Puzrin, A.M.: The bearing capacity of a strip footing on clay under combined loading, *Proc. Royal Society of London A*, 455, 893–916, 1999.

Kobayashi, S.: Hybrid type rigid plastic finite element analysis for bearing capacity characteristics of surface uniform loading, *Soils and Foundations*, 45 (2), 17–27, 2005.

Gottardi, G. & Butterfield, R.: On the bearing capacity of surface footings on sand under general planar loads, *Soils and Foundations*, 33(3), 68–79, 1993.

Poulos, H.G., Carter, J.P. & Small, J.C.: Foundations and retaining structures — Research and Practice, *Proc. 15th ICSMGE*, Istanbul, 4, 2527–2606, 2001.

Salenşon, J. & Pecker, A.: Ultimate bearing capacity of shallow foundations under inclined and eccentric loads, Part I: Purely cohesive soil, *European Journal of Mechanics A/Solids*, 14(3), 349–375, 1995.

Salenşon, J. & Pecker, A.: Ultimate bearing capacity of shallow foundations under inclined and eccentric loads, Part II: Cohesive soil without tensile strength, *European Journal of Mechanics A/Solids*, 14(3), 377–396, 1995.

Ukritchon, B., Whittle, A.J. & Sloan, S.W.: Undrained limit analysis for combined loading of strip footings on clay, *Journal of Geotechnical and Geoenvironmental Engineering*, ASCE, 124 (3), 265–276, 1998.